

Small Molecule Modulation of the Integrated Stress Response Governs the Keratoconic Phenotype In Vitro

Uri Simcha Soiberman,¹ Ahmed Elsayed Mahmoud Shehata,² Michelle Xiaoyi Lu,³ Tempest Young,³ Yassine J. Daoud,¹ Shukti Chakravarti,⁴ Albert S. Jun,¹ and James William Foster¹

¹Wilmer Eye Institute, Johns Hopkins University School of Medicine, Baltimore, Maryland, United States

²Kasr Al Ainy School of Medicine, Cairo University, Cairo, Egypt

³Johns Hopkins University, Baltimore, Maryland, United States

⁴Department of Ophthalmology, NYU Langone Health, New York, New York, United States

Correspondence: James William Foster, Wilmer Eye Institute, Smith M037, 400 North Broadway, Baltimore, MD 21231, USA; Jfoste41@jhmi.edu.

Submitted: March 26, 2019

Accepted: July 7, 2019

Citation: Soiberman US, Shehata AEM, Lu MX, et al. Small molecule modulation of the integrated stress response governs the keratoconic phenotype in vitro. *Invest Ophthalmol Vis Sci.* 2019;60:3422-3431. <https://doi.org/10.1167/iovs.19-27151>

PURPOSE. The degenerative corneal disease keratoconus is a leading indicator for corneal transplant with an unknown etiology. We recently identified the activation of the integrated stress response (ISR) in ex vivo human corneas and in vitro cell culture. Utilizing small molecules to modulate the ISR we sought to investigate the effects of stimulating the ISR in healthy cells to recapitulate aspects of the in vitro keratoconic phenotype and whether relieving the ISR signaling would recover the disease phenotype.

METHODS. Corneal fibroblasts were extracted from patients undergoing corneal transplant or unaffected cadaverous donor limbal rings. Cells were exposed to the DNA damage-inducible protein (GADD34) inhibitor SAL003 to stimulate the ISR, or Trans-ISRIB to relieve ISR signaling pathway. Collagen production was assessed through hydroxyproline production, Sirius Red incorporation, or quantitative (q)PCR. Western blotting, hydroxyproline, and qPCR were used to assess components of the ISR pathway and collagen production.

RESULTS. ISR stimulation through SAL003 resulted in significant decrease of hydroxyproline and COL1A1 transcription and eventual apoptosis in normal fibroblasts. Patient (KC) fibroblast production of hydroxyproline was increased in response to ISRIB, while matrix metalloproteinase (MMP)9 production was lowered. The prospective biomarker of keratoconus prolactin-inducible factor was also upregulated in KC fibroblast cultures in response to ISRIB. Inflammatory markers TNF α and IL-1 β were unaffected.

CONCLUSIONS. Activation of the ISR is sufficient to recapitulate many key aspects of the KC phenotype in unaffected cells in vitro. Inhibition of the ISR also relieves many of the hallmarks of KC in affected cells. Therefore, targeting of the ISR through small molecules is a potential therapeutic path for small molecule treatment of keratoconus.

Keywords: keratoconus, cell stress, collagen, ISR, ATF4

Keratoconus is a degenerative corneal disease with an incidence rate of 50 to 265 per 100,000 and onset in early adolescence.¹⁻⁴ The only available treatment for progressive keratoconus, corneal collagen crosslinking, is an effective method of slowing down or halting progression in keratoconus.⁵ However, this modality does not address the underlying biological processes that lead to disease pathogenesis, nor do other treatments aimed at visual rehabilitation, such as contact lens wear, intracorneal ring segments, or corneal transplants.⁶ Currently, there is no small molecule intervention strategy for the treatment of keratoconus either to halt or reverse the progression of this disease. We recently identified the activation of the integrated stress response (ISR) in ex vivo keratoconic corneas and in vitro human corneal fibroblasts, although the mechanism and results of this activation were not elucidated.⁷ The goal of this research was to investigate the effects of ISR modulation on normal (DN) and patient (KC) corneal fibroblasts in vitro, the hypothesis being that ISR activation in DN fibroblasts confers a keratoconic phenotype. Conversely, relief of the ISR signaling in KC fibroblasts would recover a more DN phenotype.

Previous in vitro studies have repeatedly demonstrated that reduced extracellular matrix (ECM) production is a hallmark of keratoconus fibroblasts.⁷ There are also multiple studies that have demonstrated increased production of catabolic enzymes such as matrix metalloproteinases (MMPs) in KC both in vitro and in vivo.⁸ The effects on the expression of ECM proteins, MMPs, and proteins associated with their activity in the context of the ISR have not been thoroughly investigated and have implications for understanding of the pathogenesis of diseases beyond keratoconus.

The ISR is a powerful and conserved signaling pathway that coordinates cellular responses to multiple acute and chronic intracellular and extracellular cellular stresses.^{9,10} A central node of activation is the phosphorylation of serine 51 (S51) of eukaryotic translation initiation factor 2 subunit 1 (eIF2 α); this phosphorylation leads to inhibition of eIF2B and repression of cap-dependent translation.¹¹ Accumulation of p-eIF2 α also leads to the transcription of the active uORF2 of ATF4.¹² Once translated, ATF4 translocates to the nucleus and acts as a transcription factor stimulating the production of cap-independent proteins that alter cell survival networks such as

metabolite usage,⁹ cytokine production,¹³ autophagy,¹⁴ protein folding,¹⁵ and ultimately apoptosis.¹⁶ Of note, hallmarks of keratoconus *ex vivo* and *in vitro* include altered autophagy profile, altered metabolites,¹⁷ altered cytokines,¹⁸ increased expression of protein chaperones such as CRP55, and loss of anterior stromal keratocytes.¹⁹

Critically, we have observed high levels of p-eIF2 α and nuclear ATF4 in *ex vivo* human KC corneas, although the implications of this activation were not investigated.⁷

SAL003 is a cell-permeable inhibitor of the eIF2 α phosphatase GADD34^{20,21}; this inhibition causes an increase in phosphorylated eIF2 α concentration and a nonspecific activation of the ISR. Depending on the context and duration, this activation has been shown to result in cellular adaptation and survival, or at high concentrations induction of apoptosis.²²

In contrast, the small molecule integrated stress response inhibitor and its isomer trans-ISRIB (ISRIB) have been identified as a powerful (IC₅₀ 5 nM) agonist of eIF2B by promoting the assembly of the eIF2B decamer and increasing its abundance in treated cells.^{23,24} This accumulation is posited to confer resistance to lower levels of ISR activation observed *in vivo* and *in vitro*²⁵ by restoring cellular translation capacity and relieving the cells of the effects of an active ISR.

In this study we sought to correlate our findings of the active ISR in keratoconus in an *in vitro* setting by manipulating cell cultures with SAL or ISRIB with a focus on the effects of these molecules on collagen and MMP production in primary human corneal fibroblasts.

We first investigated the effects of an active ISR on the behavior of normal corneal keratocytes (DN) to ascertain whether activation recapitulates the observed *in vitro* collagen production phenotype of keratoconus. Second, we examined whether ISRIB could rescue the stimulated (DN) or diseased (KC) phenotype. We observed that by stimulating the ISR *in vitro* we significantly decrease the production of ECM, raise the production of catabolic enzymes (MMP2), and increase the intracellular concentration of transport proteins (CALR). We observed that ISR inhibition through ISRIB was capable of partially rescuing the excessive production of MMP2 and enhanced the production of ECM proteins in multiple KC fibroblast lines. Finally, we detected that only KC fibroblasts are responsive to ISRIB especially in their active state, and that the production of COL1A1 and prolactin-induced protein (PIP), a putative KC marker, is responsive to the ISR status of the cells.²⁶ The observation that ISR modulation is sufficient to cause and relieve the symptoms of the *in vitro* KC ECM phenotype in multiple independent patient samples raises the possibility of ISR modulation being a potential therapeutic intervention in the treatment of KC.

METHODS

Ethics Statement

All human tissue was obtained under established guidelines related to informed consent for research use of human donor and patient corneas and adhered to the tenets of the Declaration of Helsinki. Informed consent was obtained from keratoconus patients using a protocol approved by the Johns Hopkins Medicine Institutional Review Board and titled "Phenotypic and Genotypic Analysis of Keratoconus" (NA_00006544). Control, healthy keratocytes were obtained from anterior stromal caps derived from healthy cadaveric corneas used for endothelial keratoplasty that are screened for keratoconus by means of anterior segment optical coherence tomography.

Cell Culture

Human stromal cells were extracted as described previously from cadaverous corneal donors (Lions Eye Bank, Baltimore, MD, USA, and Lions Eye Institute for Transplant and Research, Tampa, FL, USA), or obtained with consent from surgical samples after corneal transplantation in confirmed keratoconus patients (Wilmer Eye Institute, Baltimore, MD, USA). A total of seven individual patient cell lines were used in this study. No patients had a recorded family history of keratoconus, and patients ranged in age from 18 to 55 at the time of transplantation. Male (five) and female (two) samples were used; the reported ethnicities were Caucasian, Middle Eastern, and African American.

Briefly, epithelial and endothelial cells were removed by scraping; stromal pieces were then cut into small pieces and incubated in 1 mg/mL collagenase in fibroblast growth medium (FGM), Dulbecco's modified Eagle's medium (DMEM):F12 media containing 5% fetal bovine serum, 1 mM phosphor-ascorbic acid, 1% antibiotic/antimycotic solution (FGM) for 3 hours at 37°C. Cells were then centrifuged and released from ECM debris by treating with 0.1% trypsin/EDTA solution for 5 minutes. Trypsin was then neutralized with FGM, and the cell solution was passed through a 70- μ m cell strainer. Cells were pelleted and then resuspended in FGM and plated on tissue culture plates and allowed to divide; media were replaced every 2 or 3 days until reaching 80% confluence, after which the cells were frozen for later use or directly used for experiments. All primary cells used in the investigations detailed below were under four passages. SAL003 (PubChem ID 5717737; pubchem.ncbi.nlm.nih.gov) and Trans-ISRIB (PubChem ID 1011240) were resuspended in dimethyl sulfoxide. For serum-free culture, cells were plated and allowed to adhere overnight, media was then exchanged for a low-glucose serum-free (LGSF) media consisting of low-glucose DMEM, 1 mM phospho-ascorbic acid, 1% antibiotic/antimycotic solution, 1% insulin, transferrin, selenium (cat. no. 41400045; Thermo Fisher, Waltham, MA, USA).

Determination of Cell Number

Cell number was derived utilizing the Alamar Blue/resazurin (R7017; Sigma-Aldrich, St. Louis, MO, USA) reduction assay. A working concentration of 5.5 μ M resazurin in media was used at each media change and then incubated at 37°C for 50 minutes. The fluorescence was then measured on a fluorimeter with a 540-nm excitation and 590-nm emission; each well was read in duplicate on a fluorescent plate reader (Safire 2; Tecan, Männedorf, Switzerland) and cell number derived from standard curves of known cell number.

MMP2 and 9 Expression

Gelatin zymography was used to determine expression of MMP2 and MMP9 in response to small molecule inhibition as previously described.^{7,27} We utilized a modified zymography protocol that included the use of 2,2,2-trichloroethanol to enable the visualization of total protein prior to Coomassie blue staining to visualize gelatinases.²⁸

Total MMP Quantification

The fluorometric MMP assay (ab112146; Abcam, Cambridge, UK) was utilized to determine total MMP activity in cell culture medium. Briefly, cell culture media were preactivated with 4-aminophenylmercuric acetate for 3 hours and then incubated with the fluorescence-resonance-energy-transfer-based MMP green substrate for 1 hour. The fluorescence intensity was then

TABLE. Primer Sequences

Gene	Forward Sequence	Reverse Sequence
<i>PIP</i>	5'-CCTGCCTATGTGACGACAATCC	5'-CCTGCCTATGTGACGACAATCC,
<i>COL1A1</i>	5'-GAACGCGTGTATCCCTTGT	5'-AACGAGGTAGTCTTTTCAGCAACA
<i>MMP9</i>	5'-CAACTACGACACCGACGACC	5'-TGAATGGAAACTGGCAGGGT
<i>TIMP3</i>	5'-ACCGAGGCTTCACCAAGATGC	5'-CATCTTGCCATCATAGACGCGAC
<i>IL1B</i>	5'-CACAGACCTTCCAGGAGAATG	5'-GTGCAGTTCAGTGATCGTACAGG
<i>MMP3</i>	5'-CACTCACAGACCTGACTCGGTT	5'-AAGCAGGATCACAGTTGGCTGG
<i>MMP13</i>	5'-CTTGATGCCATTACCAGTCTCC	5'-AAACAGCTCCGCATCAACCTGC
<i>GAPDH</i>	5'-GTCTCCTCTGACTTCAACAGCG	5'-ACCACCCTGTGTCTGTAGCCAA

read on a fluorescent plate reader at Ex/Em 490/525. Average relative fluorescence units was then normalized to cell number as determined above.

Collagen Quantification

Collagen production was assayed using a modified picro-sirius red/fast green incorporation assay.²⁹ Cells were fixed for 15 minutes in 4% paraformaldehyde in PBS solution and then stained with 0.04% Fast Green (F7252; Sigma-Aldrich), dissolved in a picro-sirius red solution (STPSRPT; American Mastertech Scientific, McKinney, TX, USA) for 15 minutes. Cells were then washed three times with excess distilled water. The dyes were then eluted in 250 μ L 0.1 NaOH in methanol and absorbance at 540 and 605 nM.³⁰ Total protein and collagen were determined using the following formulas:

$$\text{Collagen} = \frac{OD540 - (OD605 \times 0.291)}{0.0378}$$

$$\text{Non-collagen} = \frac{OD605}{0.00204}$$

The 29.1% correction corresponds to the overlap between the Fast Green and Sirius Red absorbance spectrum and is required for accurate quantification. We also utilized the hydroxyproline assay to quantify collagen production by the cells. We utilized the Hydroxyproline kit (K555; BioVision, Milpitas, CA, USA) per the manufacturer's instructions. Hydroxyproline was quantified using a standard curve as directed, with values normalized to final cell number.

Western Blotting

Cells were lysed in radioimmunoprecipitation assay buffer including protease and phosphatase inhibitors; protein was run on a 10% SDS Tris-glycine gel according to standard practices. After transfer to polyvinylidene difluoride membrane, membranes were blocked with 5% nonfat dry milk (Blotto) in PBS and then incubated in blocking buffer + 0.1% Tween 20 overnight with antibodies: ATF4 (ab184909, 1:1000; Abcam), Phospho S51 eIF2 α (ab32157, 1:800; Abcam), eIF2 α (9722, 1:100; Cell Signaling Technologies, Danvers, MA, USA), CRP55 (ab92516; 1:2000; Abcam). Detection was carried out using HRP labeled antibodies and ECL.

Immunohistochemistry

Fibroblast lines were plated on eight-well chamber slides and grown in FGM overnight; cells were then dosed with SAL (2.5 μ M) or ISRIB (12.5 nM) or vehicle control for 3 days. Cells were then washed in PBS and fixed in 4% paraformaldehyde in PBS for 15 minutes. They were then permeabilized in 0.1% Triton X-100 in phosphate-buffered saline for 5 minutes. Slides were blocked in 3% FBS, 2% normal goat serum in PBS for 1 hour.

ATF4 antibody (ab184909; Abcam) was diluted in blocking buffer 1:200 and incubated overnight at 4°C. After washing 3 \times 15 minutes in PBS, secondary antibody (A-11034; Thermo Fisher) was diluted 1:500 in blocking buffer and incubated for 1 hour at room temperature. F-actin was visualized with Phalloidin, DyLight 650, (21838; Thermo Fisher) diluted 1:200 in blocking buffer was incubated for 15 minutes. Nuclei were visualized with 4',6-diamidino-2-phenylindole (DAPI). Images (\times 10) were obtained on a Zeiss Axio Imager A2 (Zeiss GMBH, Oberkochen, Germany) utilizing Axiovision software. High-magnification images were obtained on a Zeiss 510 Meta confocal microscope with a \times 63 objective utilizing Zen software.

Transcriptional Analysis by qRT-PCR

RNA was extracted using the RNeasy kit (Qiagen, Hilden, Germany) per manufacturer's instructions. Reverse transcription was carried out using the iScript cDNA Synthesis Kit (Bio-Rad, Hercules, CA, USA) with 500 ng RNA added per reaction. Quantitative (q)PCR was carried out utilizing SYBR Green standard conditions (3-step, 60°C annealing), using the CFX384 Touch Real-Time PCR machine (Bio-Rad). The primer sequences included in the Table were used. Expression was quantified using 2 $^{-\Delta\Delta C_T}$ normalized to glyceraldehyde 3-phosphate dehydrogenase and the cell line control.

Statistics

Quantitative data are presented as mean \pm SEM and were analyzed for statistical significance by unpaired, 2-tailed Student's *t*-test or 1-way ANOVA using GraphPad Prism (San Diego, CA, USA). Significance is presented as **P* < 0.5, ***P* < 0.01, ****P* < 0.001.

RESULTS

Activation of the ISR in Healthy Cells Recapitulates the In Vitro Keratoconic Phenotype

We initially tested the effects of activation on cell survival, collagen production, and expression of proteins consistent with an active ISR after 3 days in culture in serum-containing media, which promotes keratocyte proliferation. We initially undertook a toxicity assay on three independent DN cell lines and observed profound toxicity at and above 5 μ M (Fig. 1A). Analysis of the ISR pathway also demonstrated an increase in eIF2 α phosphorylation, ATF4 expression, and CRP55 expression, demonstrating a dose-dependent increase in ISR activation due to SAL003 treatment (Fig. 1B). We therefore chose the concentration of 2.5 μ M as the optimum concentration for further studies due to its lack of toxicity while still upregulating eIF2 α phosphorylation (2.4-fold), increasing ATF4 expression (>30-fold), and increasing expression of the protein

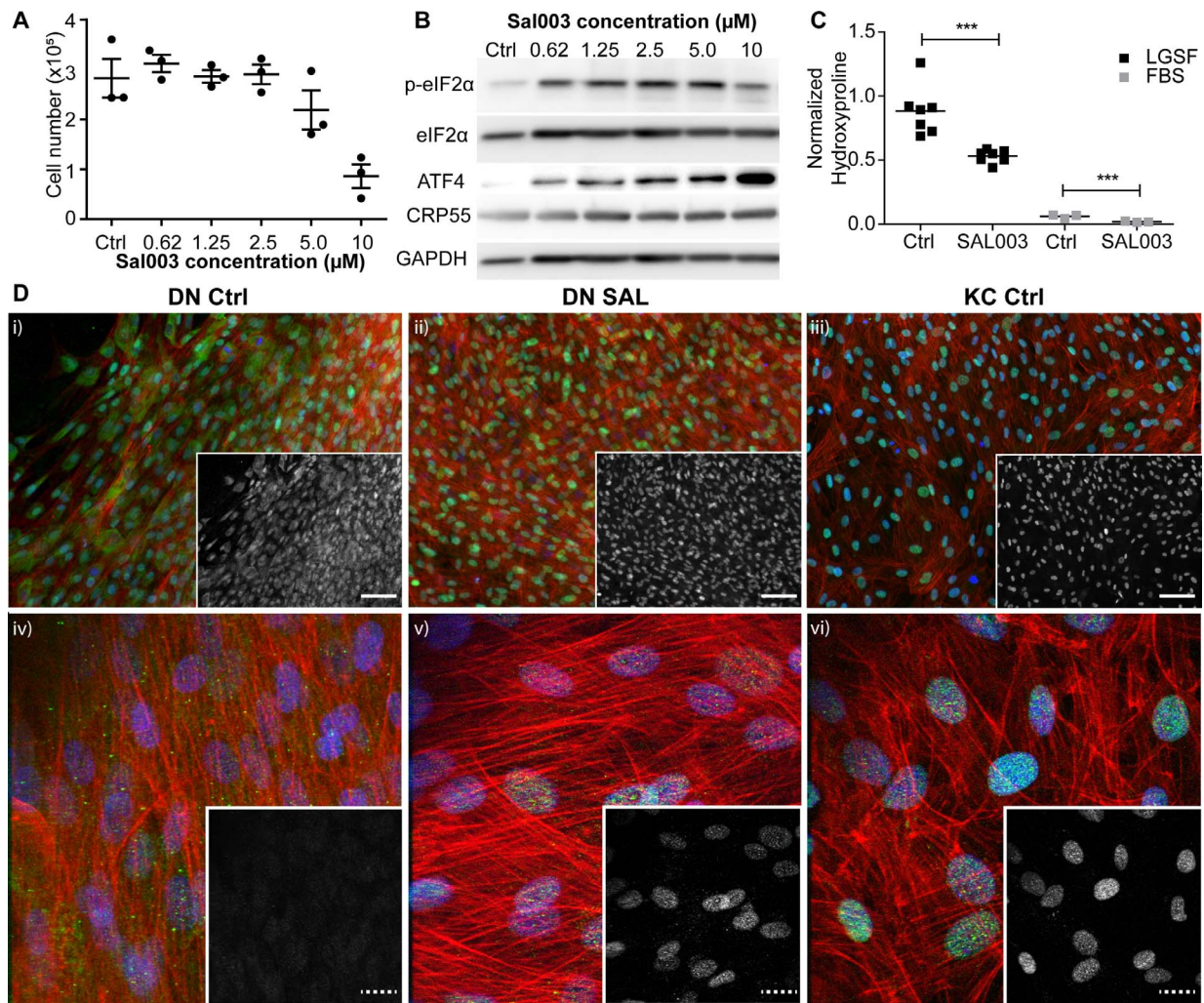


FIGURE 1. ISR activation in DN fibroblasts. **(A)** Effect of SAL003 on cell survival after 3 days of dosing in FGM media. 1×10^5 cells were seeded in FGM; the next day media were exchanged with SAL003-containing media and left for 3 days, $n = 3$. Cell number was derived by Alamar Blue reduction. The concentration 2.5 μM was determined to be the highest nontoxic dose. **(B)** Representative Western blots showing the effects of increased SAL003 concentration on eIF2 α phosphorylation, ATF4, and CRP55 expression. **(C)** Determination of collagenous protein production as measured by hydroxyproline normalized to final cell number after 7 days of culture in serum-free (LGSF), $n = 7$, or serum-containing (FGM) media, $n = 4$. **(D)** ATF4 localization in DN fibroblasts in FGM at (i) $\times 10$ magnification, (iv) $\times 63$ magnification. DN fibroblast ATF4 localization in response to 2.5 μM SAL003 treatment for 3 days at (ii) $\times 10$ magnification, (v) $\times 63$ magnification. ATF4 nuclear localization in untreated KC fibroblasts in FGM at (iii) $\times 10$ magnification, (vi) $\times 63$ magnification. *Green* and *inset*: ATF4; *red*: F-actin; *blue*: DAPI. *Solid scale bar*: 100 μm ; *dashed scale bar*: 20 μm .

chaperone CRP55 (1.8-fold), which is known to be increased in situations of high ISR signaling.³¹

A longer-duration cell culture was used to assess changes in collagen production. Specifically, collagen turnover in keratocytes, especially in quiescent cells, was found to be very slow, and therefore short-duration cultures were unlikely to produce meaningful results. However, with a 10-day culture, we observed a decrease in collagen production in SAL003-treated cells cultured in serum-containing media (FBS). FBS generally promotes keratocyte expansion, whereas culture in serum-free (LGSF) more closely recapitulates the *in vivo* quiescent keratocyte phenotype.^{7,32–34} Therefore, collagen production was assessed also in keratocytes cultured in LGSF; we observed increased collagen production (when normalized to cell number) in LGSF cultures. When treated with SAL003 for the duration of culture we observed a decrease in hydroxyproline corresponding to a $39.8 \pm 2\%$ decrease in LGSF, and a $55.13 \pm 6.8\%$ decrease in FBS relative to vehicle control (Fig. 1C). ATF4 localization, a key indicator of ISR activation, was also observed in fibroblast cultures. In DN cells, there is mixed nuclear and

cytoplasmic localization (Fig. 1D, i, iv) indicative of normal levels of ISR signaling. When treated with 2.5 μM SAL003, all ATF4 is localized to the nucleus of the cells (Fig. 1D, ii, v). For reference, the staining of control KC cells has been included, demonstrating nuclear localization (Fig. 1D, iii, vi). Individual channels and controls are included in Supplementary Figure S1.

Blocking of the ISR Can Relieve Aspects of the KC Phenotype In Vitro

The small molecule ISRIB is a potent inhibitor of the ISR, which we hypothesized would relieve some of the phenotypic changes observed in KC *in vitro* cultures. We first examined the effects of ISRIB on proliferation of KC fibroblasts over 4 days, as determined by an Alamar Blue assay (Fig. 2A). We detected no differences in doubling time in response to ISRIB dosing (50–6.25 nM), as expected. Additionally, we observed that SAL003 increased the doubling time from 26.8 ± 6.5 to 46.1 ± 13.4 hours. We assessed the effects of ISRIB on collagen

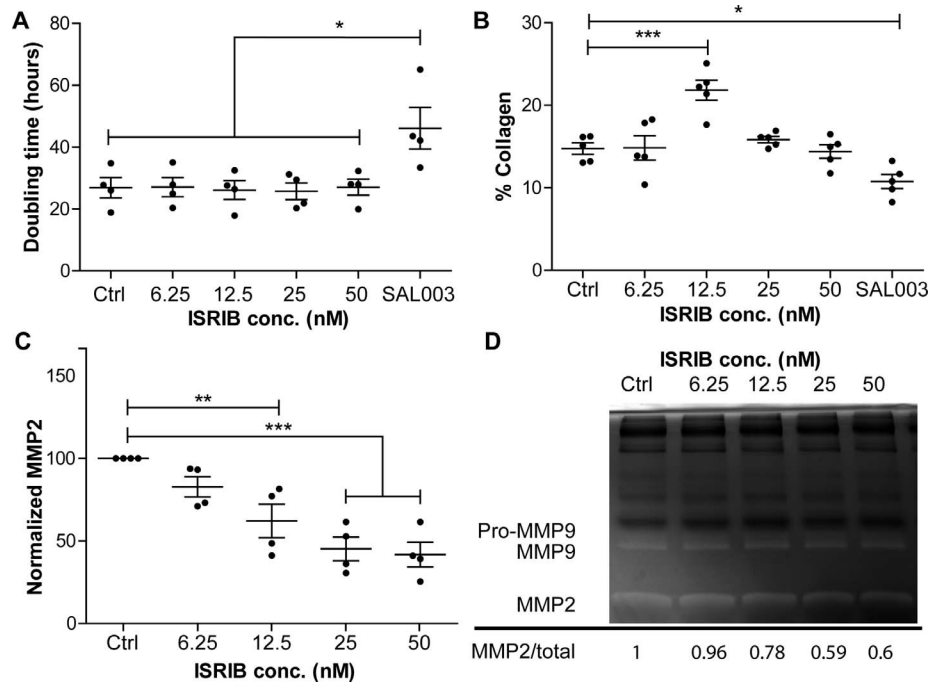


FIGURE 2. Effects of ISR inhibition on KC fibroblasts. (A) KC fibroblast doubling times in response to ISIRB dosing 50 to 6.25 nM, SAL003 (2.5 μ M included as negative control), $n = 4$. (B) Collagen production as determined by Sirius Red/Fast Green incorporation. Five individual KC fibroblast lines grown for 7 days. Values are expressed as percentage of collagenous protein (Sirius Red) divided by total protein (Fast Green) with 29.1% correction (see Methods), $N = 5$. (C) Quantification of MMP2 in response to ISIRB dosing at days 5 to 7; MMP2 was determined by gelatin zymography and normalized to Ctrl expression, $n = 4$. (D) Representative gelatin zymography of media from days 5 to 7 of culture. *Highlighted* are the MMPs 2/9; total protein is observable as the *black bands*.

production in KC keratocytes cultured in LGSF over 7 days, as determined by Sirius Red/Fast Green incorporation assay. At 12.5 nM ISIRB, we observed an increase in the percentage of collagenous proteins (Fig. 2B). As elevated MMP expression is a hallmark of KC, we examined the effects of ISIRB on the production of MMP2 as determined by gelatin zymography (Figs. 2C, 2D): When normalized to total protein we observed a dose-dependent decrease in MMP2 production (Fig. 2C). Taking all this together, we believe that 12.5 nM ISIRB is sufficient to relieve hallmark aspects of the KC ECM phenotype *in vitro*.

Investigations of MMP Production

We sought to understand the role of the ISR in regulation of MMP production; qPCR of key MMPs showed a significant increase in MMP9 transcription in KC cells relative to DN. However, no significant transcriptional differences were observed in response to either SAL or ISIRB treatments (Fig. 3A). In addition, the transcriptional levels of MMP3 and MMP13 were not affected by ISR modulation (Supplementary Fig. S3).

TIMP3, a major negative regulator of MMP activity, was shown to be significantly decreased in KC cells relative to DN cells (0.3 ± 0.2). Moreover, when treated with SAL the DN cells increased their expression (2.36 ± 0.6), whereas the KC cells barely increased their transcription to the resting levels of the DN cells (Fig. 3B). We next investigated whether the observed differences were specific to the ISR utilizing another ISR stimulating molecule, tunicamycin (TUN). Utilizing zymography we observed increased expression of MMP9 in response to both TUN (0.1 μ g/mL) and SAL (2.5 μ M) after 3 days (control [Ctrl] 0.13 ± 0.05 , TUN 9.08 ± 7.42 , SAL 1.15 ± 0.65). Importantly, the increase in MMP9 expression could be diminished when ISIRB (12.5 μ M) was included (Fig. 3C). While TUN caused an increase in MMP9 expression when

normalized to cell number, it was profoundly toxic over the 3-day cultures (Fig. 3D; Supplementary Fig. S2). Finally, we investigated the total MMP production of the cells in response to SAL, ISIRB, and in combination. Utilizing a fluorescence-based reporter assay for all MMPs we observed an increase in total MMPs in SAL-treated KC cells only (1.76 ± 0.24 to 2.75 ± 0.61), and an increased trend in DN cells, though this did not reach significance ($P = 0.18$). In contrast to the zymography results, ISIRB addition was not capable of diminishing global MMP production. We did observe that KC cells produce more constitutively active MMP species than DN (Supplementary Fig. S3), suggesting that there is a difference in MMP species being produced by the KC fibroblasts (Fig. 3E).

Differential Responses to ISR Modulation

Having demonstrated the effects of both inducing and relieving the ISR in DN and KC fibroblast cultures, we sought to investigate whether DN and KC samples would behave differently when exposed to these small molecules. We first demonstrated the effects of the different dosing regimens on the activation of the ISR in DN and KC cells (Fig. 4A). We observed that the ratio of p-eIF2 α /total eIF2 α is markedly increased in KC cells as reported previously; as expected, the addition of SAL increases phosphorylation of eIF2 α in both DN and KC cells, though this effect is increased in KC cells. ISIRB dosing reduces the p-eIF2 α ratio to levels comparable to DN. The addition of both inhibitors increases the phosphorylation of eIF2 α in both DN and KC cells, though it does appear to suppress the expression to below that of SAL alone. Utilizing qPCR, we demonstrate that COL1A1 transcription is markedly decreased in response to SAL003 dosing in both DN and KC samples (0.068 ± 0.12 , 0.16 ± 0.126 , respectively). In DN samples, ISIRB appears to marginally increase COL1A1 transcription, though this did not reach significance ($1.32 \pm$

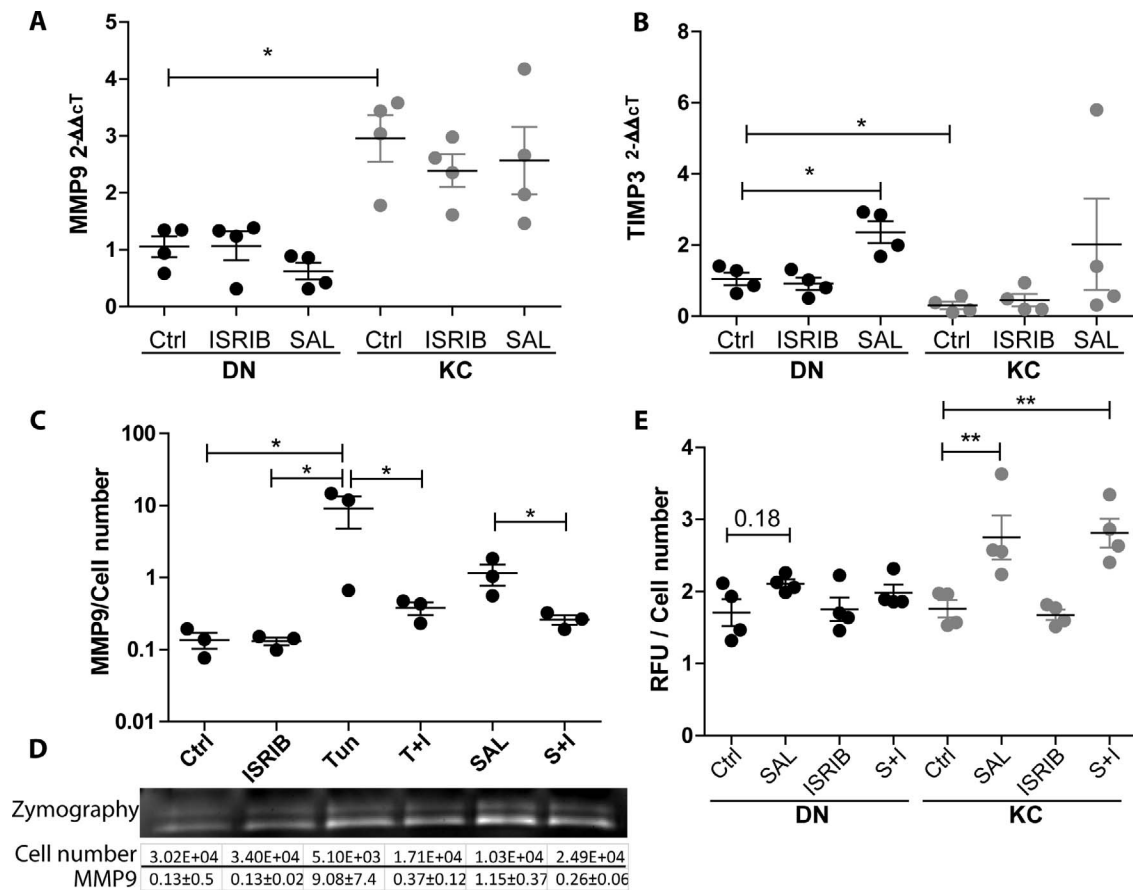


FIGURE 3. MMP response to ISR modulation. (A) MMP9 transcription in response to ISR modulation is unchanged yet KC cells have increased overall levels relative to DN Ctrl. (B) TIMP3 transcription is decreased in KC relative to DN. SAL treatment causes an increase in DN cells only, which is not significantly different from DN Ctrl samples. (C) MMP9 expression as measured by gelatin zymography relative to final cell number; 0.1 μ M TUN and SAL both increase MMP9 expression. Addition of ISRIB to either TUN (T+I) or SAL (S+I) reduces expression and preserves cell viability, $n = 3$. (D) Representative zymogram and average quantification of MMP9 expression and cell number. (E) Results of total MMP quantification in response to ISR modulation relative to cell number after 3 hours of 4-aminophenylmercuric acetate activation, $n = 4$. KC cells show increased total MMP production in response to SAL and S+I treatment.

0.162-fold). However, in the KC samples we see significant upregulation of COL1A1 (from 0.88 ± 0.28 to 1.25 ± 0.24 -fold), suggesting that ISRIB was capable of relieving the key hallmark of in vitro KC cultures, low collagen production (Fig. 4B). Utilizing hydroxyproline we observed a dose-dependent increase in response to ISRIB (DN 32%, KC 35%) and a corresponding decrease in response to SAL003 (DN 27%, KC 39%), in broad agreement with the qPCR results (Fig. 4C). We also sought to investigate whether an active ISR could stimulate expression of proinflammatory markers as there are well-reported changes in cytokines in the keratoconic eye. Analysis of IL-1 β showed that both DN and KC fibroblasts have barely detectable levels of IL-1 β transcription at baseline or when treated with ISRIB (Fig. 4D). However, when exposed to SAL there is an increased trend of IL-1 β transcription in both DN and KC cells ($P = 0.08, 0.12$). TNF α expression was also assayed in the media and found to be barely detectable in most samples (Supplementary Fig. S5).

Finally, we investigated the expression of a candidate KC biomarker, the hormone prolactin-induced protein (PIP), which has been described as being reduced in KC patients, though the mechanism causing this reduction is unknown.²⁷ Here we demonstrated that activation of the ISR in DN cells causes a decrease in transcription (0.19 ± 0.14). In contrast, blocking of the ISR through ISRIB in KC cells is sufficient to increase the transcription of PIP in vitro (0.57 ± 0.33 - to 1.32 ± 0.38 -fold)

(Fig. 3E). Based on the data presented here we therefore believe that ISR activation underlies a majority of the previously described aspects of the KC in vivo and in vitro phenotypes.

DISCUSSION

We have previously described the activation of the ISR as a key hallmark of KC ex vivo and in vitro, although the causes and effects of this activation were unknown. In this study we sought to investigate the effects of ISR modulation on the behavior of healthy and diseased corneal fibroblasts to test the hypothesis that ISR activation could cause, and inhibition could recover, the in vitro ECM keratoconic phenotype. Utilizing the GADD34 inhibitor SAL003 in DN cells, we have determined the optimal dosing concentration to activate the ISR and trigger a KC-like phenotype, namely, decreased collagen production, increased MMP2, nuclear localization of ATF4, and increased CRP55.⁷ We then demonstrated that attenuation of the ISR through the small molecule ISRIB is sufficient to increase the collagen production of KC fibroblasts while decreasing the production of MMP2 while having little effect on DN cells. We believe that this is due to the constitutive activation of the ISR in KC cells alone.

We also observed complex regulation of MMPs and their inhibitory proteins in response to the ISR. The transcriptional

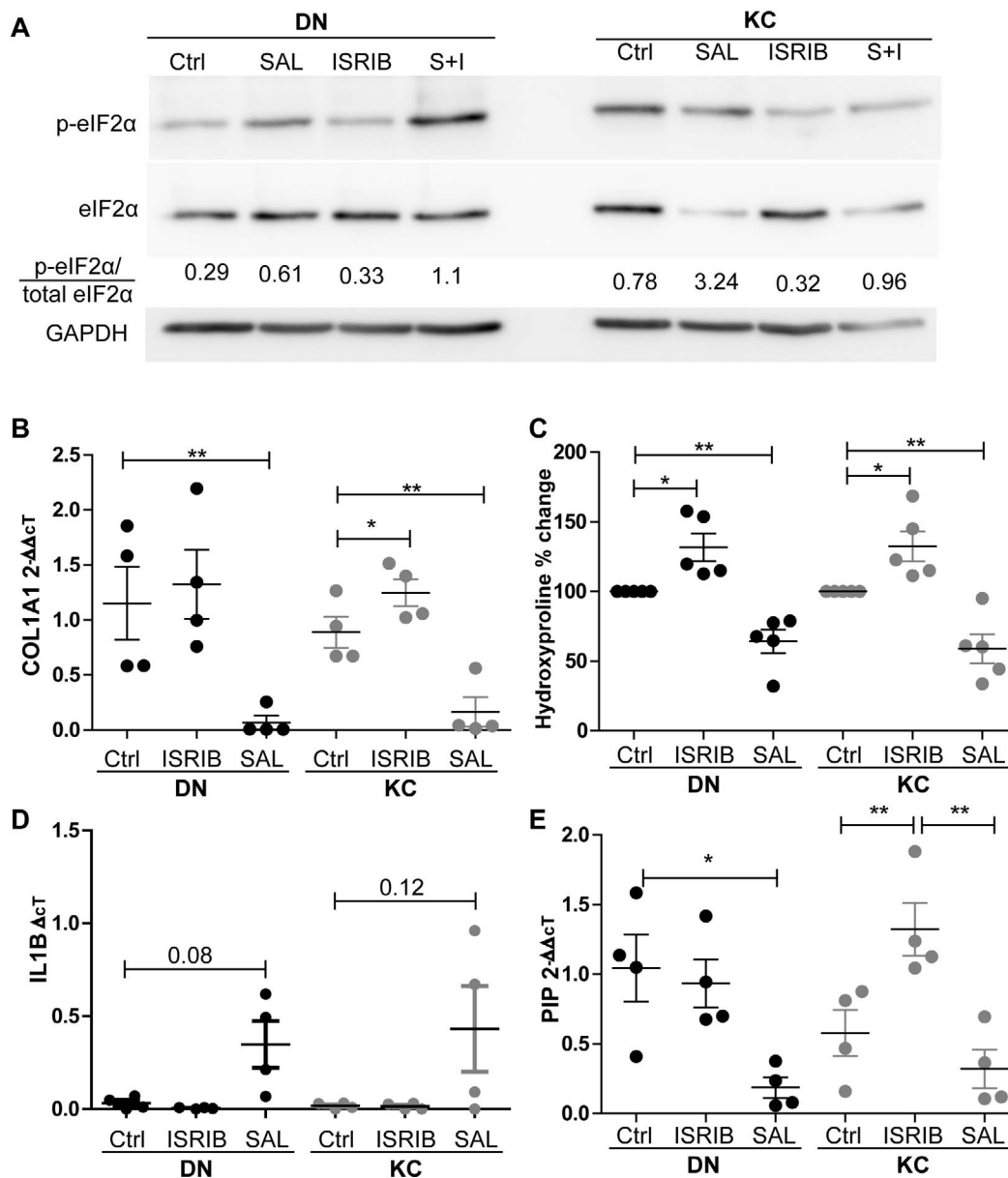


FIGURE 4. Differential response to ISR modulation. (A) Representative Western blots showing effects of ISR modulation with SAL, ISRIB, or SAL+ISRIB (S+I) on eIF2 α phosphorylation over 3 days in serum-containing culture. (B) COL1A1 transcriptional levels in response to ISR stimulation or inhibition, $n = 4$. DN and KC fibroblasts grown for 7 days in serum-free media with either vehicle control, ISRIB (12.5 nM), or SAL003 (2.5 μ M). (C) Quantification of hydroxyproline production in response to ISRIB and SAL003. Hydroxyproline production was normalized to final cell number and plotted as percentage change relative to vehicle, $n = 5$. (D) Transcriptional levels of IL-1 β in response to ISR stimulus values are plotted as $\Delta\Delta$ ct with undetectable samples given the expression value of 0. (E) Expression of the putative KC marker PIP increase in transcription was only observed in KC cells in response to ISRIB while SAL003 caused a decrease in both DN and KC cells.

levels of several MMPs were unaffected by initiation of the ISR, whereas TIMP3, an inhibitor of MMP activity and a protein that has been previously reported as being underexpressed in KC corneas, was not stimulated in KC cells as it was in DN cells.³⁵ This complex regulation of MMPs was also apparent when we investigated the global MMP expression levels, with SAL stimulating profound increases in total MMPs in KC cells only. Further investigations will focus on identifying those MMP species that are most responsive to the ISR stimulus.

Finally, we demonstrate that the effects of ISR modulation are specific to diseased cells, with ISRIB stimulating increased COL1A1 transcription and hydroxyproline production in KC cells only. We also investigated the expression of prospective inflammatory cytokines IL-1 β and TNF α , which have been

described as being dysregulated in keratoconus.³⁶ We observed that both IL-1 β and TNF α were not produced above the detection threshold by DN or KC fibroblasts under untreated conditions and, although there was a trend toward increased expression (by qPCR and ELISA), in both cases the levels of expression were barely above the detection threshold. As these cytokines and others have been reported in KC previously, this suggests that the increased levels observed are from other cell types. We also observed that the putative KC biomarker PIP is responsive to the ISR, and that stimulation in DN cells (recapitulating KC) is sufficient to suppress its transcription as is observed in the disease. Conversely in KC cells, relief of the ISR signaling with ISRIB is sufficient to cause an increase in its transcription.

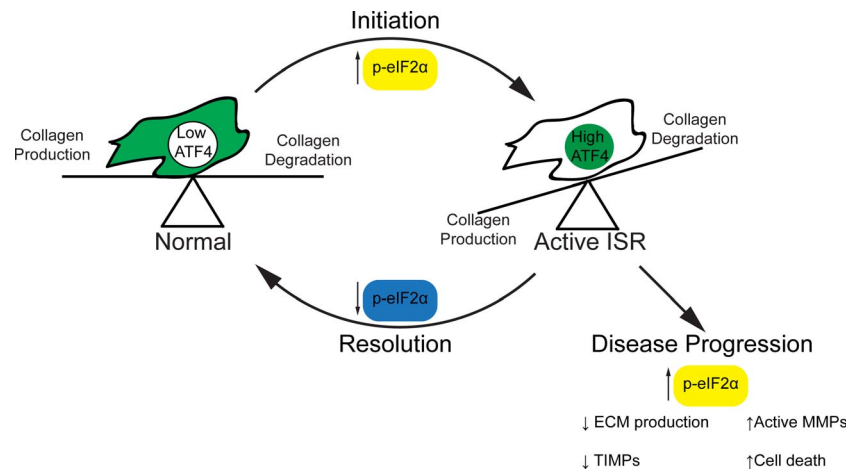


FIGURE 5. Hypothesized role of the ISR in regulation of keratoconus. In the unaffected cornea, homeostasis is maintained between collagen production and degradation and the uORF2 of ATF4 is not expressed. Upon stimulation of the ISR, p-eIF2 α increases in concentration and triggers a transient decrease in collagen production. Upon resolution of the stressor, p-eIF2 α concentrations return to normal and homeostasis is restored. In the patient, p-eIF2 α remains high and there is a consistent decrease in collagen production. The amount of active MMPs is also increased and ECM degradation continues, leading to failure of the tissue.

The activation of the ISR has been associated with the pathogenesis of several diseases not related to the cornea, including Alzheimer's disease, diabetes mellitus, and several retinopathies. However, these investigations have been focused on the role of highly metabolically active cells rather than on fibroblasts. We believe that the corneal stroma is uniquely exposed to all the triggers that have been reported in the activation of the ISR: heme-regulated inhibitor kinase (HRI) in response to heme deficiency or oxidative stress,³⁷ protein kinase R (PKR) in response to double-strand RNA (viruses),³⁸ PERK (EIF2AK3) in response to the unfolded protein response and hypoxia,³⁹ and GCN2 (EIF2AK4) in response to amino acid deprivation or UV light.⁴⁰ Findings and observations that could conceivably affect all four of these kinases have been documented in the cornea; the presence of hemosiderin in Fleischer rings as an example of heme dysfunction,⁴¹ exposure to the environment as a source of pathogens and UV light, blinking and sleep as a source of hypoxia, and the unique way in which nutrients are delivered to the cornea as a source of nutrient deprivation.⁴² Based on our previous results,⁷ we believe that the unfolded protein response is a key driver of KC as we were able to exclude differences based on three of the four kinases within our *in vitro* model. Specifically, we observed persistence of signaling *in vitro* where extracellular sources of stimulation had been removed.

Although ISR stimulation can be achieved through multiple small molecules,⁴³ we sought to use the cell-permeable analogue of salubrinal, SAL003, to stimulate the ISR through accumulation of p-eIF2 α . This was based on our own experience with the other small molecule TUN, which is highly toxic (<0.1 μ g/mL) over the duration of cultures studied here. We hypothesized that in KC, ISR activity can be caused by additive effects of activation from more than one of the ISR activating kinases; therefore SAL003 treatment would recapitulate the broadest spectrum of disease, although the nature of the ISR stimulation is still elusive and may well be different across the spectrum of patients.

The "cascade hypothesis" of keratoconus suggested that abnormal lipids and nitric oxide cause accumulation of cytotoxic components that trigger the apoptosis of keratocytes and the failure of the tissue.⁴⁴ The interplay between redox state and the ISR has been described previously in other cell types,^{11,45} although the results seem to be dependent on context. The results presented here support this hypothesis

that intracellular stress is a leading driver of keratoconus progression.

Interestingly, the observation that MMP9 transcriptional levels are unaffected by ISR activation may lead to further understanding of the cascade to failure seen in KC. Under normal homeostasis the turnover of the cornea is balanced between degradation, mostly by MMPs, and collagen production. However, in the context of an active ISR this axis is tilted toward degradation. As the ECM is a major reservoir of inactive MMPs, this change in homeostasis may be sufficient to cause release and activation of these catabolic enzymes, setting up the runaway failure that is characteristic of the disease (Fig. 5). Indeed, it is only at the final stages of the disease that new collagen, in the form of scarring, is identified.⁴⁶

Further investigations will focus on determining the status and nature of the unfolded protein response within patient populations. Of note is that none of the patients from which the KC fibroblasts were derived reported a family history of KC, further complicating the search for the triggers of the disease. However, these results showed consistency across the diverse patient population tested and correlate with several findings from the literature on the nature of the KC ECM phenotype. Therefore, if perturbation of the ISR pathway in KC fibroblasts proves to be nontoxic *in vivo* and the *in vitro* effects persist, targeting of the ISR in KC patients could provide an avenue of investigation for pharmacological intervention in the disease.

Acknowledgments

Supported by The Marfan Foundation's Victor A. McKusick Fellowship Program (JWF), a Research to Prevent Blindness departmental grant (JWF), a generous donation from the Small family (JWF), National Institutes of Health Grant K08EY027474 (USS), and EY026104 (SC).

Disclosure: U.S. Soiberman, None; A.E.M. Shehata, None; M.X. Lu, None; T. Young, None; Y.J. Daoud, None; S. Chakravarti, None; A.S. Jun, None; J.W. Foster, None

References

- Soiberman U, Foster JW, Jun AS, Chakravarti S. Pathophysiology of keratoconus: what do we know today. *Open Ophthalmol J.* 2017;11:252-261.

2. Rabinowitz YS. Keratoconus. *Surv Ophthalmol.* 1998;42: 297-319.
3. Godefrooij DA, de Wit GA, Uiterwaal CS, Imhof SM, Wisse RPL. Age-specific incidence and prevalence of keratoconus: a nationwide registration study. *Am J Ophthalmol.* 2017;175: 169-172.
4. Woodward MA, Blachley TS, Stein JD. The association between sociodemographic factors, common systemic diseases, and keratoconus. *Ophthalmology.* 2016;123:457-465.
5. Hersh PS, Stulting RD, Muller D, Durrie DS, Rajpal RK; United States Crosslinking Study Group. United States multicenter clinical trial of corneal collagen crosslinking for keratoconus treatment. *Ophthalmology.* 2017;124:1259-1270.
6. Bergmanson JPG, Goosey JD, Patel CK, Mathew JH. Recurrence or re-emergence of keratoconus - what is the evidence telling us? Literature review and two case reports. *Ocul Surf.* 2014;12:267-272.
7. Foster JW, Shinde V, Sioberman US, et al. Integrated stress response and decreased ECM in cultured stromal cells from keratoconus corneas. *Invest Ophthalmol Vis Sci.* 2018;59: 2977-2986.
8. Kenney MC, Chwa M, Oprobek AJ, Brown DJ. Increased gelatinolytic activity in keratoconus keratocyte cultures. A correlation to an altered matrix metalloproteinase-2/tissue inhibitor of metalloproteinase ratio. *Cornea.* 1994;13:114-124.
9. Harding HP, Zhang Y, Zeng H, et al. An integrated stress response regulates amino acid metabolism and resistance to oxidative stress. *Mol Cell.* 2003;11:619-633.
10. Taniuchi S, Miyake M, Tsugawa K, Oyadomari M, Oyadomari S. Integrated stress response of vertebrates is regulated by four eIF2 α kinases. *Sci Rep.* 2016;6:32886.
11. Pavitt GD. Regulation of translation initiation factor eIF2B at the hub of the integrated stress response. *Wiley Interdiscip Rev RNA.* 2018;9:e1491.
12. Dey S, Baird TD, Zhou D, Palam LR, Spandau DF, Wek RC. Both transcriptional regulation and translational control of ATF4 are central to the integrated stress response. *J Biol Chem.* 2010;285:33165-33174.
13. Martinon F, Glimcher LH. Regulation of innate immunity by signaling pathways emerging from the endoplasmic reticulum. *Curr Opin Immunol.* 2011;23:35-40.
14. B'chir W, Maurin A-C, Carraro V, et al. The eIF2 α /ATF4 pathway is essential for stress-induced autophagy gene expression. *Nucleic Acids Res.* 2013;41:7683-7699.
15. Bernard-Marissal N, Moumen A, Sunyach C, et al. Reduced calreticulin levels link endoplasmic reticulum stress and Fas-triggered cell death in motoneurons vulnerable to ALS. *J Neurosci.* 2012;32:4901-4912.
16. Armstrong JL, Flockhart R, Veal GJ, Lovat PE, Redfern CPF. Regulation of endoplasmic reticulum stress-induced cell death by ATF4 in neuroectodermal tumor cells. *J Biol Chem.* 2010; 285:6091-6100.
17. Karamichos D, Zieske J, Sejersen H, Sarker-Nag A, Asara JM, Hjortdal J. Tear metabolite changes in keratoconus. *Exp Eye Res.* 2015;132:1-8.
18. Balasubramanian SA, Mohan S, Pye DC, Willcox MDP. Proteases, proteolysis and inflammatory molecules in the tears of people with keratoconus. *Acta Ophthalmol.* 2012;90: e303-e309.
19. Kim WJ, Rabinowitz YS, Meisler DM, Wilson SE. Keratocyte apoptosis associated with keratoconus. *Exp Eye Res.* 1999;69: 475-481.
20. Gao B, Zhang X, Han R, et al. The endoplasmic reticulum stress inhibitor salubrinal inhibits the activation of autophagy and neuroprotection induced by brain ischemic preconditioning. *Acta Pharmacol Sin.* 2013;34:657-666.
21. Choy MS, Yusoff P, Lee IC, et al. Structural and functional analysis of the GADD34:PP1 eIF2 α phosphatase. *Cell Rep.* 2015;11:1885-1891.
22. Zeng N, Li Y, He L, et al. Adaptive basal phosphorylation of eIF2 α is responsible for resistance to cellular stress induced cell death in Pten null hepatocytes. *Mol Cancer Res.* 2011;12: 1708-1717.
23. Zyryanova AF, Weis F, Faille A, et al. Binding of ISRIB reveals a regulatory site in the nucleotide exchange factor eIF2B. *Science.* 2018;359:1533-1536.
24. Sidrauski C, McGeachy AM, Ingolia NT, Walter P. The small molecule ISRIB reverses the effects of eIF2 α phosphorylation on translation and stress granule assembly. *Elife.* 2015;4: e05033.
25. Rabouw HH, Langereis MA, Anand AA, et al. Small molecule ISRIB suppresses the integrated stress response within a defined window of activation. *Proc Natl Acad Sci U S A.* 2019; 116:2097-2102.
26. Sharif R, Bak-Nielsen S, Hjortdal J, Karamichos D. Pathogenesis of keratoconus: the intriguing therapeutic potential of prolactin-inducible protein. *Prog Retin Eye Res.* 2018;67:150-167.
27. Toth M, Fridman R. Assessment of gelatinases (MMP-2 and MMP-9) by gelatin zymography. *Methods Mol Med.* 2001;57: 163-174.
28. Raykin J, Snider E, Bheri S, Mulvihill J, Ethier CR. A modified gelatin zymography technique incorporating total protein normalization. *Anal Biochem.* 2017;521:8-10.
29. Segnani C, Ippolito C, Antonioli L, et al. Histochemical detection of collagen fibers by Sirius Red/Fast Green is more sensitive than van Gieson or Sirius Red alone in normal and inflamed rat colon. *PLoS One.* 2015;10:e0144630.
30. López-De León A, Rojkind M. A simple micromethod for collagen and total protein determination in formalin-fixed paraffin-embedded sections. *J Histochem Cytochem.* 1985;33: 737-743.
31. Michalak M, Corbett EF, Mesaeli N, Nakamura K, Opas M. Calreticulin: one protein, one gene, many functions. *Biochem J.* 1999;344:281-292.
32. Foster JW, Gouveia RM, Connon CJ. Low-glucose enhances keratocyte-characteristic phenotype from corneal stromal cells in serum-free conditions. *Sci Rep.* 2015;5:10839.
33. Gouveia RM, Connon CJ. The effects of retinoic acid on human corneal stromal keratocytes cultured in vitro under serum-free conditions. *Invest Ophthalmol Vis Sci.* 2013;54: 7483-7491.
34. Borderie VM, Mourra N, Laroche L. Influence of fetal calf serum, fibroblast growth factors, and hepatocyte growth factor on three-dimensional cultures of human keratocytes in collagen gel matrix. *Graefes Arch Clin Exp Ophthalmol.* 1999;237:861-869.
35. Lee J-E, Oum BS, Choi HY, Lee SU, Lee JS. Evaluation of differentially expressed genes identified in keratoconus. *Mol Vis.* 2009;15:2480-2487.
36. Ionescu IC, Corbu CG, Tanase C, et al. Overexpression of tear inflammatory cytokines as additional finding in keratoconus patients and their first degree family members. *Mediators Inflamm.* 2018;2018:4285268.
37. Uma S, Yun B-G, Matts RL. The heme-regulated eukaryotic initiation factor 2 α kinase: a potential regulatory target for control of protein synthesis by diffusible gases. *J Biol Chem.* 2001;276:14875-14883.
38. Dey M, Cao C, Dar AC, et al. Mechanistic link between PKR dimerization, autophosphorylation, and eIF2 α substrate recognition. *Cell.* 2005;122:901-913.
39. Teske BF, Wek SA, Bunpo P, et al. The eIF2 kinase PERK and the integrated stress response facilitate activation of ATF6

- during endoplasmic reticulum stress. *Mol Biol Cell*. 2011;22:4390-4405.
40. Deval C, Chaveroux C, Maurin A-C, et al. Amino acid limitation regulates the expression of genes involved in several specific biological processes through GCN2-dependent and GCN2-independent pathways. *FEBS J*. 2009;276:707-718.
 41. McPherson SD, Kiffney GT. Some histologic findings in keratoconus. *Arch Ophthalmol*. 1968;79:669-673.
 42. Duane TD. Metabolism of the cornea. *Arch Ophthalmol*. 1949;41:736-749.
 43. Liu L, Qi X, Chen Z, et al. Targeting the IRE1 α /XBP1 and ATF6 arms of the unfolded protein response enhances VEGF blockade to prevent retinal and choroidal neovascularization. *Am J Pathol*. 2013;182:1412-1424.
 44. Cristina Kenney M, Brown DJ. The cascade hypothesis of keratoconus. *Cont Lens Anterior Eye*. 2003;26:139-146.
 45. Kitiphongspattana K, Khan TA, Ishii-Schrade K, Roe MW, Philipson LH, Gaskins HR. Protective role for nitric oxide during the endoplasmic reticulum stress response in pancreatic beta-cells. *Am J Physiol Endocrinol Metab*. 2007;292:E1543-E1554.
 46. Zadnik K, Barr JT, Edrington TB, et al. Corneal scarring and vision in keratoconus: a baseline report from the Collaborative Longitudinal Evaluation of Keratoconus (CLEK) Study. *Cornea*. 2000;19:804-812.